CHIN. PHYS. LETT. Vol. 38, No. 5 (2021) 057501

Itinerant Topological Magnons in *SU(2)* Symmetric Topological Hubbard Models with Nearly Flat Electronic Bands

Zhao-Long Gu(顾昭龙)[1] and Jian-Xin Li(李建新)[1,2*]

[1]*National Laboratory of Solid State Microstructures and Department of Physics, Nanjing University, Nanjing 210093, China*
[2]*Collaborative Innovation Center of Advanced Microstructures, Nanjing University, Nanjing 210093, China*

(Received 7 February 2021; accepted 23 March 2021; published online 2 May 2021)

We show that a suitable combination of flat-band ferromagnetism, geometry and nontrivial electronic band topology can give rise to itinerant topological magnons. An $SU(2)$ symmetric topological Hubbard model with nearly flat electronic bands, on a Kagome lattice, is considered as the prototype. This model exhibits ferromagnetic order when the lowest electronic band is half-filled. Using the numerical exact diagonalization method with a projection onto this nearly flat band, we can obtain the magnonic spectra. In the flat-band limit, the spectra exhibit distinct dispersions with Dirac points, similar to those of free electrons with isotropic hoppings, or a local spin magnet with pure ferromagnetic Heisenberg exchanges on the same geometry. Significantly, the non-flatness of the electronic band may induce a topological gap at the Dirac points, leading to a magnonic band with a nonzero Chern number. More intriguingly, this magnonic Chern number changes its sign when the topological index of the electronic band is reversed, suggesting that the nontrivial topology of the magnonic band is related to its underlying electronic band. Our work suggests interesting directions for the further exploration of, and searches for, itinerant topological magnons.

DOI: 10.1088/0256-307X/38/5/057501

Band structures with nontrivial topology[1] have been at the forefront of condensed matter physics since the discovery of topological insulators.[2,3] Although pioneering works focused primarily on fermionic systems,[4−9] the underlying concepts of band topology, such as the Berry phase or Berry curvature,[10] Chern number,[11,12] and Dirac or Weyl points,[13] are independent of the statistics of the constituent quasiparticles, and can therefore be generalized to systems with bosonic elementary excitations. In recent years, much effort has been devoted to the exploration of, and searches for, topological magnons,[14−32] i.e., the bosonic quanta of collective spin-1 excitations with nontrivial band structures in magnetically ordered systems, not only in the context of a fundamental interest in physical terms, but also due to their possible applications in spintronics.[33]

Typical theoretical proposals[15,19] relating to topological magnons include ferromagnetic Heisenberg models on the Kagome or honeycomb lattices, together with special spin-exchange interactions, such as the Dzyaloshinskii–Moriya (DM) terms.[34,35] In the context of linear spin wave theory,[36] which maps the magnetically ordered spin system to a free bosonic version, the generation of nontrivial magnonic band topology can be better understood in parallel to its free electronic counterpart. On the Kagome and honeycomb lattices, pure ferromagnetic Heisenberg models exhibit Dirac magnons at the corners of the Brillouin zone, due to the symmetries of the lattice geometries. The presence of the DM term would introduce magnon hoppings with complex amplitudes, leading to effective staggered flux on the lattice. As a result, the Dirac magnons would be gapped, and the magnonic band would acquire a nonzero Chern number, identical to its electronic counterpart. Such a scheme has been tested on several Kagome and honeycomb ferromagnets by the direct measurement of magnon dispersions in inelastic neutron scattering experiments.[16,29]

While the bulk of research into topological magnons is based on local spin models, it has been found quite recently that topological magnons could also emerge in itinerant magnets.[31,32] In one of our previous works,[32] we demonstrated the first theoretical realization of two-dimensional (2D) itinerant topological magnons, based on the quarter-filled Haldane–Hubbard model on the honeycomb lattice, with a nearly flat electronic band. However, with this as our only example, the guiding principle for finding itinerant topological magnons remains unclear. On the other hand, due to the lack of even one specific local electronic spin per physical site, the linear spin-wave theory fails for itinerant magnons, and no standard analytical framework exists for studying band topol-

Supported by the National Natural Science Foundation of China (Grant No. 11774152), and National Key R&D Program of China (Grant No. 2016YFA0300401).
*Corresponding author. Email: jxli@nju.edu.cn
© 2021 Chinese Physical Society and IOP Publishing Ltd

ogy. Therefore, new physical insights are required for any further investigation or understanding of itinerant topological magnons.

In this Letter, we show that itinerant topological magnons would result from a suitable combination of flat-band ferromagnetism, geometry, and nontrivial electronic band topology, based on an alternative example of 2D itinerant topological magnons, and symmetry arguments. The prototype is an $SU(2)$ symmetric topological Hubbard model, with nearly flat electronic bands on the Kagome lattice. This model exhibits ferromagnetic order when the lowest electronic band is hall-filled. Using a numerically exact diagonalization method with a projection onto this nearly flat band, we obtain the magnonic spectra. The spectra display two prominent features. Firstly, in the flat-band limit, the spectra exhibit distinct dispersions with Dirac points, similar to those of free electrons with isotropic hoppings, or a local spin magnet with pure ferromagnetic Heisenberg exchanges on the same geometry. Secondly, the non-flatness of the electronic band could induce a nontrivial gap in the Dirac magnons, resulting in a magnonic band with a nonzero Chern number. As such, the non-flatness of the electronic band plays a similar role in the generation of nontrivial band topology to that of complex hoppings in the free electronic model, or DM interaction in the local-spin ferromagnet. Furthermore, this magnonic Chern number changes its sign when the topological index of the electronic band is reversed, suggesting that the nontrivial topology of the magnonic band is in some sense inherited from its underlying electronic band. These features are quite generic for flat-band ferromagnets realized on nontrivial electronic bands, and arguably result from the symmetries of such models. Our work sheds new light on the exploration of, and the search for, itinerant topological magnons.

The Hamiltonian, $\hat{H}$, of the $SU(2)$ symmetric Hubbard model with topological electronic bands on the Kagome lattice can be expressed as

$$\hat{H} = t_1 \sum_{\langle ij\rangle\sigma} c^{\dagger}_{i\sigma} c_{j\sigma} + \text{H.c.} + t_2 \sum_{\langle\langle ij\rangle\rangle\sigma} c^{\dagger}_{i\sigma} c_{j\sigma} + \text{H.c.} + \lambda \sum_{\langle ij\rangle\sigma} e^{\phi_{ij}} c^{\dagger}_{i\sigma} c_{j\sigma} + \text{H.c.} + U \sum_{i} n_{i\uparrow} n_{i\downarrow}. \quad (1)$$

Here, $\langle ij\rangle$ and $\langle\langle ij\rangle\rangle$ denote the nearest-neighbor (NN) and next-nearest-neighbor (NNN) bonds, respectively, and $\phi_{ij} = \pm\phi$ is the phase of the NN hopping, with the sign given by the solid green arrows in Fig. 1(a). Other parameters are given as per standard notation.

Since there are three inequivalent sites in the unit cell of a Kagome lattice [see Fig. 1(a)], the free part of Eq. (1) hosts three energy bands, each of which is two-fold degenerate, due to the spin's degrees of freedom. When $\lambda = 0$, or $\phi = 0$, as shown in Fig. 2(a), the middle band touches the lower band at the K/K' points, forming two inequivalent Dirac points at the corners of the Brillouin zone [see Fig. 1(b)]. Moreover, the middle band and the upper band are degenerate at the Γ point. When both λ and ϕ take nonzero values, staggered flux is generated on the Kagome lattice, and all the degeneracies between different bands are removed. As a result, as shown in Fig. 2(b), the Dirac points are gapped, and both lower and upper energy bands acquire nonzero Chern numbers.

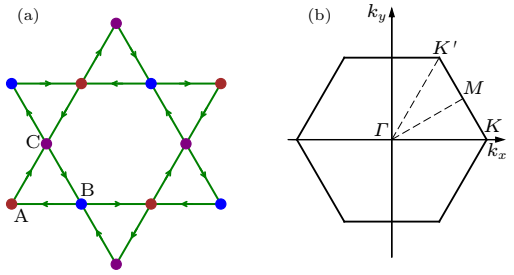

Fig. 1. (a) Illustration of complex hopping amplitudes on the Kagome lattice, where A, B, and C denote the three inequivalent sites within a unit cell. (b) The Brillouin zone.

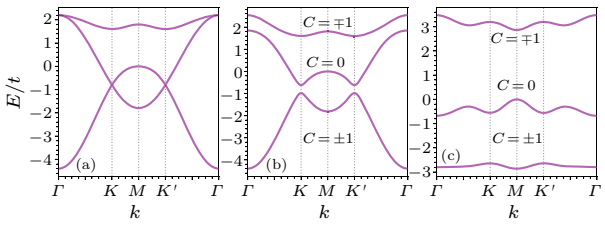

Fig. 2. Electronic energy bands of the free part of Eq. (1): (a) $t_1 = -1.0$, $t_2 = -0.1$, $\phi = 0$, $\lambda = 0$, (b) $t_1 = -1.0$, $t_2 = -0.1$, $\phi = \frac{\pi}{2}$, $\lambda = \pm 0.1$, and (c) $t_1 = -1.0$, $t_2 = 0.3$, $\phi = \frac{\pi}{2}$, $\lambda = \pm 0.6$. In (b) and (c), depending on the sign of λ, the Chern numbers in the lower electronic bands are ± 1, with the middle bands being 0, and the upper bands being ∓ 1.

Given appropriate tuning of the hopping parameters, these three separated energy bands could become quite flat [see Fig. 2(c)]. In the past decade or so, nearly flat topological bands have attracted much attention, owing to the fact that exotic topological phases of matter, such as fractional Chern insulators, can be stabilized in a fractionally filled nearly flat topological band in the presence of strong interactions, even at high temperatures.[37–43] In this study, however, we focus on the case in which the lower, nearly flat electronic band is half-filled; with a strong enough Hubbard interaction (typically larger than the bandwidth of the lower electronic band), the ground state comprises a ferromagnetic state with fully polarized spin,[32,44–48] which exhibits an integer quantum Hall effect.[49] In such a phase, the degrees of freedom of electron charge are frozen, and spin excitations dominate the low-energy physics.

The fully spin-polarized ferromagnetic state in the Kagome lattice can be written as $|\text{FM}\rangle \equiv$

$\prod_{\boldsymbol{k}\in \mathrm{BZ}} d^{\dagger}_{\boldsymbol{k}\uparrow}|0\rangle$. Here, $|0\rangle$ denotes the vacuum for electrons, and $d^{\dagger}_{\boldsymbol{k}\uparrow}$ creates a spin-up electron, with a momentum $\boldsymbol{k}$ in the lower electronic band. Generally speaking, the dimension of the Hilbert space of spin-1 excitations over the $|\mathrm{FM}\rangle$ state scales exponentially with an increase in system size, N, making the resolution of spin-1 excitation spectra impossible, even numerically, for a system with hundreds of sites. Fortunately, when the Hubbard interaction strength, U, does not exceed the gap between the lower and middle electronic bands (i.e., the parameter region constituting our area of focus in this work), the system can be projected onto the lower electronic band. A basis for spin-1 excitations with a center-of-mass momentum $\boldsymbol{q}$ can then be written as $|\boldsymbol{k}_i\rangle_{\boldsymbol{q}} = d^{\dagger}_{\boldsymbol{k}_i-\boldsymbol{q}\downarrow} d_{\boldsymbol{k}_i\uparrow}|\mathrm{FM}\rangle$. It appears that the dimension of this set of bases simply scales linearly with N.[31,32,48] With this projection, a much larger system can be numerically accessed. In the following, the magnonic spectra are actually calculated for a system with a size of $N = 60 \times 60$.

The matrix element of the projected Hamiltonian $P\hat{H}P$ on this set of bases is

$$ {}_{\boldsymbol{q}}\langle \boldsymbol{k}_j|P^{\dagger}\hat{H}P|\boldsymbol{k}_i\rangle_{\boldsymbol{q}} = [M^1_i(\boldsymbol{q}) + M^2_i(\boldsymbol{q})]\delta_{\boldsymbol{k}_j,\boldsymbol{k}_i} - M^3_{ji}(\boldsymbol{q}), \tag{2}$$

where P is the projector onto the lower electronic band, and

$$M^1_i(\boldsymbol{q}) = \varepsilon_d(\boldsymbol{k}_i - \boldsymbol{q}) - \varepsilon_d(\boldsymbol{k}_i), \tag{3}$$

$$M^2_i(\boldsymbol{q}) = \frac{U}{N}\sum_{a=A,B,C}\sum_{\boldsymbol{p}} |\mu_{a\boldsymbol{p}\uparrow}|^2 |\mu_{a\boldsymbol{k}_i-\boldsymbol{q}\downarrow}|^2, \tag{4}$$

$$M^3_{ji}(\boldsymbol{q}) = \frac{U}{N}\sum_{a=A,B,C} \mu^*_{a\boldsymbol{k}_i-\boldsymbol{q}\downarrow}\mu_{a\boldsymbol{k}_i\uparrow}\mu_{a\boldsymbol{k}_j-\boldsymbol{q}\downarrow}\mu^*_{a\boldsymbol{k}_j\uparrow}. \tag{5}$$

Here, $\varepsilon_d(\boldsymbol{k})$ denotes the dispersion of the lower electronic band, and $\mu_{a\boldsymbol{k}\sigma}$ $(a = A, B, C)$ is the probability amplitude of the sublattice, a, which contributes to the lower electronic band, $d_{\boldsymbol{k}\sigma} = \sum_{a=A,B,C}\mu_{a\boldsymbol{k}\sigma}c_{a\boldsymbol{k}\sigma}$. The $M^1(\boldsymbol{q})$ term in Eq. (2) results from the non-flatness of the lower electronic band, while the $M^2(\boldsymbol{q})$ and $M^3(\boldsymbol{q})$ terms result from Hubbard interaction. We note that, for the topological Hubbard model considered in this study, $M^2(\boldsymbol{q}) \equiv \frac{U}{3}$. This is because the Hamiltonian, $\hat{H}$, preserves the three-fold rotation symmetry that permutes the A, B and C sublattices; thus, for the lower electronic band, $\sum_{\boldsymbol{p}}|\mu_{A\boldsymbol{p}\uparrow}|^2 = \sum_{\boldsymbol{p}}|\mu_{B\boldsymbol{p}\uparrow}|^2 = \sum_{\boldsymbol{p}}|\mu_{C\boldsymbol{p}\uparrow}|^2 \equiv \frac{N}{3}$, and then $M^2_i(\boldsymbol{q}) = \frac{U}{N}\sum_{a=A,B,C}\frac{N}{3}|\mu_{a\boldsymbol{k}_i-\boldsymbol{q}\downarrow}|^2 = \frac{U}{3}$.

We begin with the spin-1 excitation spectra in the flat-band limit, which are obtained by setting the $M^1(\boldsymbol{q})$ term in Eq. (2) to zero. The results, based on three typical λ values, are presented in Figs. 3(a1)–3(c1). The spectra consist of two parts: the low-lying spin waves, indicated by the green lines, and the high-energy Stoner continuum, denoted by the grey lines located at $U/3$ [about 0.67 in Figs. 3(a1)–3(c1), since at that location, $U = 2.0$]. The spin waves contain three branches of well-defined magnonic bands, and their dispersions are quite similar to the electronic energy bands shown in Fig. 2(a). Here, the spectra exhibit three major features. Firstly, the lower magnonic band is gapless at the Γ point, as guaranteed by the Goldstone theorem, because the ground state simultaneously breaks the spin rotation symmetry from $SU(2)$ to $U(1)$, and develops a typical ferromagnetic quadratic dispersion from this point. Secondly, the lower magnonic band touches the middle one at the K/K' points. Thirdly, the middle and upper magnonic bands are degenerate at the Γ point. Both the second and third features mentioned above are also characteristic of the energy bands of free fermions with isotropic hoppings [see Fig. 2(a)].

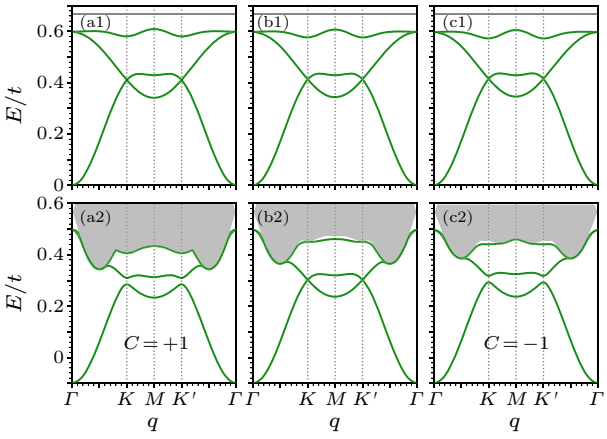

Fig. 3. Spin-1 excitation spectra of a 1/6 filled $SU(2)$ topological Hubbard model on the Kagome lattice, where (a1)–(c1) are in the flat-band limit, and (a2)–(c2) are for the case that the non-flatness of the lower electronic band considered. The Chern number of the lower magnonic band in (a2) is $+1$, while that in (c2) is -1. The parameters are (a) $\lambda = 0.6$, (b) $\lambda = 0.625$, and (c) $\lambda = 0.65$. Other parameters are fixed at $t_1 = -1.0$, $t_2 = 0.3$, $\phi = \frac{\pi}{2}$, and $U = 2.0$.

Next, we study the effects of the non-flatness of the lower electronic band on the magnonic spectra. The results for the same model parameters as given in Figs. 3(a1)–(c1), but with the $M^1(\boldsymbol{q})$ term included, are presented in Figs. 3(a2)–(c2). At first glance, the spectra are only moderately modified, which is consistent with the fact that the bandwidth of the lower electronic band is smaller than the Hubbard interaction, so that the $M^1(\boldsymbol{q})$ term could be considered as a perturbation. However, the nonflatness of the lower electronic band actually gives rise to nontrivial effects. In this case, the Stoner continuum extends from a horizontal line to a wide energy range with dispersive boundaries, touches the middle and upper magnonic bands, and distorts their dispersions at the area of contact. More intriguingly, the Dirac magnons at the K/K' points are now gapped, with the exception of some fine-tuned model parameters

[e.g., Fig. 3(b2)], leading to a topologically nontrivial lower magnonic band with a nonzero Chern number. By varying the dispersion of the lower electronic band, this magnonic Chern number can be reversed from $C = +1$ [Fig. 3(a2)] to $C = -1$ [Fig. 3(c2)] by means of a gap-closing point [Fig. 3(b2)]. We note that the Chern number of the lower electronic band remains unchanged (i.e., is always 1) during this process. Generally speaking, the non-flatness of the lower electronic band can therefore be deemed to play a similar role to the λ term [the third term in Eq. (1)] in the generation of nontrivial band topology [see Fig. 2(b)] and the Chern number of the magnonic band could be either the same as, or opposite to, that of its underlying electronic band. Furthermore, we note that the non-flatness of the lower electronic band cannot remove the degeneracy between the middle and the upper magnonic bands at the Γ point for all model parameters, because at $\boldsymbol{q} = 0$, the $M^1(\boldsymbol{q})$ term in Eq. (2) vanishes identically [see Eq. (3)].

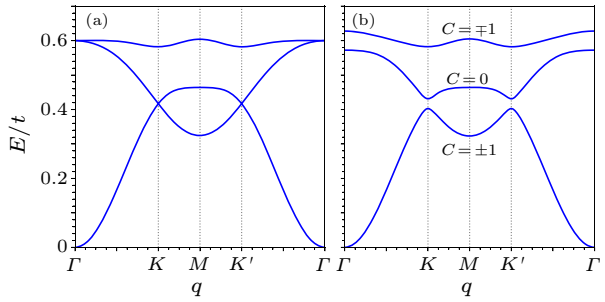

Fig. 4. Spin wave excitations of the ferromagnetic Heisenberg model (a) without and (b) with ($A = \pm 0.008$), where the nearest-neighbor DM interaction on the Kagome lattice is calculated via the linear spin-wave theory. In (b), depending on the sign of A, the Chern number of the lower magnonic band is ± 1, with 0 for the middle band, and ∓ 1 for the upper band. The other parameters are $J_1 = -0.085$, $J_2 = -0.015$, and $J_3 = -0.008$.

The band structure of the itinerant topological magnons on the Kagome lattice is not only analogous to free electrons with both isotropic and complex hoppings on the same geometry, but also to the ferromagnetic Heisenberg model with the nearest-neighbor DM interaction, whose Hamiltonian, $\hat{H}_S$, can be written as $\hat{H}_S = \hat{H}_H + \hat{H}_{\rm DM}$, where $\hat{H}_H$ denotes the Heisenberg component:

$$\hat{H}_H = J_1 \sum_{\langle ij \rangle} \boldsymbol{S}_i \cdot \boldsymbol{S}_j + J_2 \sum_{\langle\langle ij \rangle\rangle} \boldsymbol{S}_i \cdot \boldsymbol{S}_j + J_3 \sum_{\langle\langle\langle ij \rangle\rangle\rangle} \boldsymbol{S}_i \cdot \boldsymbol{S}_j, \tag{6}$$

and $\hat{H}_{\rm DM}$ is the DM interaction,

$$\hat{H}_{\rm DM} = A \sum_{\langle ij \rangle} [\boldsymbol{S}_i \times \boldsymbol{S}_j]_z. \tag{7}$$

In order to present this analogy more clearly, in Fig. 4, we plot the magnonic bands of this model, calculated using the linear spin-wave theory, for comparison. As shown in Fig. 4(a), with appropriate tuning of the J_1, J_2, and J_3 parameters, the spin-wave bands of the pure Heisenberg model perfectly simulate the magnonic bands of the itinerant ferromagnet in the flat-band limit, apart from the Stoner continuum [see Fig. 3(a)], which is the unique feature of itinerant magnetism. When the DM interaction strength, A, is not zero, as shown in Fig. 4(b), the degenerate points of the three magnonic bands are removed, and the lower band acquires a nonzero Chern number, similar to the phenomenon observed in Figs. 3(a2) and 3(c2).

Based on the numerical results, we have demonstrated that three quite different systems, i.e., itinerant flat-band ferromagnets, free electronic models, and local spin ferromagnets, could share quite similar band structures in terms of their respective elementary excitations. Between the free electronic models and local spin ferromagnets, this similarity is already well-understood, by virtue of standard linear spin wave theory. However, the underlying reason for the similarity between itinerant flatband ferromagnets and either one of the others remains elusive. Here, we attempt to provide a phenomenological understanding, based on symmetry arguments. If we approximate the itinerant magnons solved by the numerical method as free bosons, they can also hop on the Kagome lattice in real space. In the flat-band limit, the hoppings of these free magnons are primarily determined by the Hubbard interaction, i.e., the $M^2(\boldsymbol{q})$ and $M^3(\boldsymbol{q})$ terms in Eq. (2). Due to the $SU(2)$ spin rotation symmetry of the model, and the isotropic nature of the Hubbard interaction, the magnon hoppings should also be isotropic in real space in this case. When the non-flatness of the lower electronic band is considered, extra magnon hopping terms would appear, owing to the additional $M^1(\boldsymbol{q})$ term in Eq. (2). However, the $M^1(\boldsymbol{q})$ term merely represents the difference between the eigenvalues of free electrons with different momenta; an inverse Fourier transformation from momentum space to real space should result in a hopping term for the magnons that shares the same pattern as the λ term for electrons, whose amplitude can be positive, zero, or negative, depending on the values of $M^1(\boldsymbol{q})$. Here this amplitude is nonzero, the Dirac magnons at the K/K' points will be gapped, and the lower magnonic band will acquire a nonzero Chern number, whose sign is determined by that of the amplitude. At the same time, the point where the amplitude equals zero is effectively a transition point, across which the magnonic Chern number changes its sign. Based on this argument, we infer that the nontrivial band topology of the itinerant magnons is to a certain extent inherited from that of its underlying electronic band. This argument could be further

supported by the fact (verified by our numerical results) that the magnonic Chern number changes its sign when the topological index of the lower electronic band is reversed.

In summary, we have demonstrated that itinerant topological magnons can result from a suitable combination of flat-band ferromagnetism, geometry, and nontrivial electronic band topology. The prototype is an $SU(2)$ symmetric topological Hubbard model with nearly flat electronic bands, on a Kagome lattice. This model exhibits ferromagnetic order when the lowest electronic band is half-filled. The magnonic spectra over this ferromagnetic ground state acquires two prominent features: firstly, in the flat-band limit, the spectra exhibit distinct dispersions with Dirac points, similar to those of the free electronic model, or a local spin ferromagnet on the same geometry. Secondly, the non-flatness of the electronic band can induce a nontrivial gap in the Dirac magnons, resulting in a magnonic band with a nonzero Chern number. Furthermore, this magnonic Chern number changes its sign when the topological index of the electronic band is reversed, suggesting that the nontrivial topology of the magnonic band is in some sense inherited from its underlying electronic band.

Based on the symmetry arguments, the observed properties of the magnonic spectra of itinerant magnons in the flatband ferromagnets realized on nearly flat topological electronic bands are quite generic. Our work may provide guidance for future research into itinerant topological magnons.

References

[1] Bansil A, Lin H and Das T 2016 *Rev. Mod. Phys.* **88** 021004
[2] Hasan M Z and Kane C L 2010 *Rev. Mod. Phys.* **82** 3045
[3] Qi X L and Zhang S C 2011 *Rev. Mod. Phys.* **83** 1057
[4] Haldane F D M 1988 *Phys. Rev. Lett.* **61** 2015
[5] Kitaev A Y 2001 *Phys. Usp.* **44** 131
[6] Kane C L and Mele E J 2005 *Phys. Rev. Lett.* **95** 226801
[7] Bernevig B A, Hughes T L and Zhang S C 2006 *Science* **314** 1757
[8] Qi X L, Hughes T L, Raghu S and Zhang S C 2009 *Phys. Rev. Lett.* **102** 187001
[9] Yu S L, Xie X C and Li J X 2011 *Phys. Rev. Lett.* **107** 010401
[10] Berry M V 1984 *Proc. R. Soc. A* **392** 45
[11] Thouless D J, Kohmoto M, Nightingale M P and den Nijs M 1982 *Phys. Rev. Lett.* **49** 405
[12] Simon B 1983 *Phys. Rev. Lett.* **51** 2167
[13] Wan X, Turner A M, Vishwanath A and Savrasov S Y 2011 *Phys. Rev. B* **83** 205101
[14] Onose Y, Ideue T, Katsura H, Shiomi Y and Nagaosa N 2010 *Science* **329** 297
[15] Zhang L, Ren J, Wang J S and Li B 2013 *Phys. Rev. B* **87** 144101
[16] Chisnell R, Helton J, Freedman D, Singh D and Bewley R 2015 *Phys. Rev. Lett.* **115** 147201
[17] Li F Y, Li Y D, Kim Y B, Balents L and Yu Y 2016 *Nat. Commun.* **7** 12691
[18] Mook A, Henk J and Mertig I 2016 *Phys. Rev. Lett.* **117** 157204
[19] Owerre S A 2016 *J. Phys.: Condens. Matter* **28** 386001
[20] Roldán-Molina A, Nunez A S and Fernández-Rossier J 2016 *New J. Phys.* **18** 045015
[21] Malki M and Schmidt K P 2017 *Phys. Rev. B* **95** 195137
[22] Su Y, Wang X S and Wang X R 2017 *Phys. Rev. B* **95** 224403
[23] Laurell P and Fiete G A 2017 *Phys. Rev. Lett.* **118** 177201
[24] McClarty P A, Krger F, Guidi T, Parker S F and Refson K 2017 *Nat. Phys.* **13** 736
[25] Mook A, Henk J and Mertig I 2017 *Phys. Rev. B* **95** 014418
[26] Li K, Li C, Hu J, Li Y and Fang C 2017 *Phys. Rev. Lett.* **119** 247202
[27] Yao W, Li C, Wang L, Xue S and Dan Y 2018 *Nat. Phys.* **14** 1011
[28] Bao S, Wang J, Wang W, Cai Z and Li S 2018 *Nat. Commun.* **9** 2591
[29] Chen L, Chung J H, Gao B, Chen T and Stone M B 2018 *Phys. Rev. X* **8** 041028
[30] Pershoguba S S, Banerjee S, Lashley J *et al.* 2018 *Phys. Rev. X* **8** 011010
[31] Su X F, Gu Z L, Dong Z Y and Li J X 2018 *Phys. Rev. B* **97** 245111
[32] Gu Z L, Dong Z Y, Yu S L and Li J X 2019 arXiv:1908.09255 [cond-mat.str-el]
[33] Chumak A V, Vasyuchka V I, Serga A A and Hillebrands B 2015 *Nat. Phys.* **11** 453
[34] Dzyaloshinsky I 1958 *J. Phys. Chem. Solids* **4** 241
[35] Moriya T 1960 *Phys. Rev.* **120** 91
[36] Holstein T and Primakoff H 1940 *Phys. Rev.* **58** 1098
[37] Tang E, Mei J W and Wen X G 2011 *Phys. Rev. Lett.* **106** 236802
[38] Wang F and Ran Y 2011 *Phys. Rev. B* **84** 241103
[39] Sun K, Gu Z, Katsura H and Sarma S D 2011 *Phys. Rev. Lett.* **106** 236803
[40] Wang Y F, Gu Z C, Gong C D and Sheng D N 2011 *Phys. Rev. Lett.* **107** 146803
[41] Neupert T, Santos L, Chamon C and Mudry C 2011 *Phys. Rev. Lett.* **106** 236804
[42] Sheng D N, Gu Z C, Sun K and Sheng L 2011 *Nat. Commun.* **2** 389
[43] Regnault N and Bernevig B A 2011 *Phys. Rev. X* **1** 021014
[44] Tasaki H 1992 *Phys. Rev. Lett.* **69** 1608
[45] Mielke A 1993 *Phys. Lett. A* **174** 443
[46] Mielke A and Tasaki H 1993 *Commun. Math. Phys.* **158** 341
[47] Doretto R L and Goerbig M O 2015 *Phys. Rev. B* **92** 245124
[48] Su X F, Gu Z L, Dong Z Y, Yu S L and Li J X 2019 *Phys. Rev. B* **99** 014407
[49] Neupert T, Santos L, Ryu S, Chamon C and Mudry C 2012 *Phys. Rev. Lett.* **108** 046806